Desantes Fernández, JM.; Benajes Calvo, JV.; García Martínez, A.; Monsalve Serrano, J. (2014). The role of the in-cylinder gas temperature and oxygen concentration over low load reactivity controlled compression ignition combustion efficiency. Energy. 78:854-868. doi:10.1016/j.energy.2014.10.080.

The Role of the In-Cylinder Gas Temperature and Oxygen Concentration over Low Load RCCI Combustion Efficiency

José M. Desantes, Jesús Benajes, Antonio García*, Javier Monsalve-Serrano

CMT - Motores Térmicos, Universitat Politècnica de València, Camino de Vera s/n, 46022 Valencia, Spain

(*) CORRESPONDING AUTHOR:

Dr. Antonio Garcia: angarma8@mot.upv.es

Telephone: +34 963879659

Fax: +34 963877659

ABSTRACT

Several studies carried out with the aim of improving the RCCI concept in terms of thermal efficiency conclude that the main cause of the reduced efficiency at light loads is the reduced combustion efficiency. The present study used both a 3D computational model and engine experiments to explore the effect of the oxygen concentration and intake temperature on RCCI combustion efficiency at light load. The experiments were conducted using a single-cylinder heavy-duty research diesel engine adapted for dual fuel operation.

Results suggest that it is possible to achieve an improvement of around 1.5% in the combustion efficiency with both strategies studied; the combined effect of intake temperature and in-cylinder fuel blending as well as the combined effect of oxygen concentration and in-cylinder fuel blending (ICFB). In addition, the direct comparison of both strategies suggests that the combustion losses trend is mainly associated to the in-cylinder equivalence ratio stratification, which is determined by the diesel to gasoline ratio in the blend since the injection timing is kept constant for all the tests. Moreover, the combined effect of the intake temperature and ICFB promotes a slight improvement in the combustion losses over the combined effect of the oxygen concentration and ICFB.

KEYWORDS

RCCI

Low load

Combustion efficiency

EURO VI

Oxygen concentration

Intake temperature

1. INTRODUCTION

Since decades, internal combustion engines (ICE) play a fundamental role in the society. The capability of the ICEs to cover fundamental requirements such as people and goods transportation and power generation, has result in their mass production. Due to the extensive use of the ICEs, stringent regulations are being introduced around the world to limit their pollutant emissions with the aim of reducing their environmental impact. In addition, a prime requirement by the users is to improve the fuel economy, which in turn results in higher ICE efficiency. In this sense, the higher compression ratio (CR), un-throttled operation and shorter combustion duration of the compression ignition (CI) engines than the spark ignition (SI) engines offers a greater potential to increase the thermal efficiency. In spite of its potential, the rich local equivalences ratios, high temperatures achieved during a conventional mixing-controlled diesel combustion in CI diesel engines as well as the oxygen availability in the outside of the spray plume results in a unacceptable NOx and soot emissions, taking into account the current regulations such as EURO VI. Soot emissions can be reduced by using a DPF, which requirement of regeneration results in a fuel consumption penalty. Since TWC achieves their maximum efficiency operating with equivalence ratios near stoichiometric or slight richer, a poor NOx reduction efficiency is obtained. Thus, NOx emissions can be minimized through the use of a LNT or SCR technology requiring periodically regeneration (operating rich) and the introduction of a reducing agent respectively, which worsens the fuel consumption. In order to reduce aftertreatment costs and fuel consumption it is necessary to avoid the generation of these pollutants in the focus of the emission, i.e. during the combustion development. In this sense, the automotive scientific community and manufacturers are currently focusing part of their efforts on the investigation of new combustion modes [1][2] and on the optimization of the current technology with the purpose of reducing fuel consumption and engine-out emissions.

The more promising combustion strategies to simultaneously improve the engine efficiency while reducing the most relevant diesel engine-out emissions, NOx and soot, under the

regulation limits are the low temperature combustion (LTC) strategies. LTC strategies are based on promoting a lean air-fuel mixture together with a low temperature combustion avoiding the NOx and soot formation. The efficiency is improved as a consequence of the fast heat release obtained when the proper in-cylinder conditions are achieved, as well as the reduction in heat transfer (HT) losses due to the lower in-cylinder temperature peaks. In this sense, the well-known combustion concept based on fully premixed lean mixtures Homogeneous Charge Compression Ignition (HCCI) [3][4] has been widely investigated. Although HCCI achieves important emission benefits [5], this combustion concept presents some practical issues that must be solved before it can be implemented in CI diesel engines, which limit the HCCI operating range to low engine speeds and loads [6]. The most relevant limitations consist of achieving an appropriate combustion phasing, cycle-to-cycle control of the combustion process, spray impingements and its effects on the emissions [7], combustion noise and operating range extent. Several techniques such as EGR [8], variable valve timing [9][10], variable compression ratio [11] and intake air temperature variation [12] have been investigated in order to overcome these drawbacks. Due to the high chemical reactivity of the diesel fuel, the mentioned techniques cannot provide precise control over the combustion phasing since they require large time scales to achieve cycle-to-cycle control. Thus, when increasing engine load not enough mixing time before the start of combustion is provided. On this regard, Bessonette et al. [13] suggested that different in-cylinder reactivity is required for the proper HCCI operation under different operating conditions. Specifically, high cetane fuels are required at low load and a low cetane fuels are needed at medium-high load.

In order to improve the controllability and widen the engine operating range, Partially Premixed Combustion (PPC) strategy has been studied. This LTC strategy is based on reduce the air-fuel mixing degree by injecting later in the cycle than in HCCI strategy, attaining an in-cylinder equivalence ratios stratification. The strategy offers higher control on the ignition delay as well as the combustion duration, which depends on the partial stratification of the

fuel provided by the injection timing. In addition, lower in-cylinder pressure gradients are obtained reducing the knocking level. Despite their benefits, as in HCCI strategy, the use of diesel fuel [14] requires high levels of EGR when increasing engine load to achieve a proper combustion phasing [15], which reduces the thermal efficiency. In order to avoid this shortcomings, the use of fuels with lower reactivity [16][17][18][19][20] than diesel fuel (lower cetane number) such as gasoline has been proposed. The use of gasoline provides more flexibility to achieve the required extra mixing time at medium-high loads [21]. Several studies confirmed gasoline PPC as a promising method to control the heat release rate providing a reduction in NOx and soot emissions [19][22][23]. However, the concept has demonstrated difficulties at low load conditions [24][25] using gasoline with octane number greater than 90, concluding that the use of a low reactivity fuel under PPC conditions provide some control on combustion phasing but still do not offers the possibility of cycle-to-cycle control. Thus, it seems that additionally to the equivalence ratio stratification, an in-cylinder PRF stratification will be required to proper operating LTC strategies at different operating conditions.

Reactivity Controlled Compression Ignition (RCCI) combustion allows both sources of stratification (equivalence ratio and PRF) by direct in-cylinder blending different reactivity fuels. To delivery both fuels separate injection systems for the low-reactivity and high-reactivity fuel are used, being port fuel injected (PFI) and direct injected (DI) respectively. Thus, a flexible operation over a wide operating range is possible by modifying both, the low reactivity fuel percentage in the blend and the direct injection timing. Recent experimental and simulated studies confirm that RCCI concept allows an effective ignition control and a low maximum PRR (pressure rise rate) while maintaining low engine-out emissions levels and high fuel efficiency simultaneously, proving that the RCCI concept is a more promising LTC technique than HCCI [26] and PPC. In this sense, Kokjohn et al. [27] and Splitter et al. [28] studied RCCI combustion over a wide range of engine loads and conditions concluding that the main cause of the reduced efficiency at light loads is the reduced combustion efficiency. Thus,

it is possible to achieve combustion efficiencies near 98% by reducing the combustion losses, which is considered an acceptable value for a premixed combustion strategy. The main objective of the present work is to evaluate the coupled effect of the in-cylinder gas temperature or oxygen concentration with the in-cylinder fuel blending ratio on RCCI combustion losses (CO and unburned HC) in a heavy-duty (HD) CI engine. For this purpose EGR and intake temperature sweeps have been carried out. Both sweeps (intake temperature and EGR) have been performed keeping constant the combustion phasing (CA50) by adjusting the gasoline percentage in the blend as required in each case and keeping constant the rest of the engine settings. In addition two constraints have been taken into account for the tests: NOx and soot under EURO VI limits for HD diesel engines (NOx <0.4 g/kWh and soot <0.01 g/kWh) and ringing intensity (RI) below 5 MW/m^2, which was established by Dec and Yang [29] as a proper upper limit to achieve an acceptable combustion noise and knock-free operation. In addition to the experimental tests, a computational analysis by means of a CFD code has been conducted in order to better explain the results.

2. EXPERIMENTAL FACILITIES AND PROCESSING TOOLS

2.1 Test cell and engine description

A single cylinder, HD diesel engine representative of commercial truck engine, has been used for all experiments in this study. Detailed specifications of the engine are given in Table 1.

The engine was installed in a fully instrumented test cell, with all the auxiliary facilities required for its operation and control, as it is illustrated in Figure 1. Moreover, to achieve stable intake air conditions, a screw compressor supplied the required boost pressure before passing through an air dryer. The air pressure was adjusted within the intake settling chamber, while the intake temperature was controlled in the intake manifold after mixing with EGR. The exhaust backpressure produced by the turbine in the real engine was replicated by means of a valve placed in the exhaust system, controlling the pressure in the exhaust settling chamber.

Low pressure EGR was produced taking exhaust gases from the exhaust settling chamber. Then, once it was filtered by a DPF, its temperature was reduced passing through a heat exchanger. After that, water steam and condensate were separated from gas by means of a centrifugal filter, and resulting gases were passed through a secondary filter. Furthermore, a roots-type supercharger was used in order to provide the external EGR mass flow rate desired. With the aim of lowering the gas temperature increase caused by the supercharger, a second heat exchanger was used before the arrival of the EGR gases to a settling chamber equipped with an electric heater. It was then introduced into the intake pipe, closing the external EGR loop. The temperature regulation was performed upon the EGR-fresh air mixture, by means of a temperature sensor in the intake manifold. Finally, the exact EGR rate was controlled by means of a valve between the EGR settling chamber and the intake pipe. The determination of the EGR rate was carried out using the experimental measurement of intake and exhaust CO_2 concentration. The concentrations of NOx, CO, unburned HC, intake and exhaust CO_2, and O_2 were analyzed with a five gas Horiba MEXA-7100 DEGR analyzer bench by averaging 40 seconds after attaining steady state operation. CO and unburned HC measurements were used to determine the combustion efficiency as:

$$\mathbf{Comb.Eff} = \left(\mathbf{1} - \frac{\mathbf{HC}}{\mathbf{mf}} - \frac{\mathbf{CO}}{\mathbf{4 \cdot mf}}\right) \cdot \mathbf{100}$$

Smoke emission were measured with an AVL 415S Smoke Meter and averaged between three samples of a 1 liter volume each with paper-saving mode off, providing results directly in FSN (Filter Smoke Number) units. PM measurements of FSN were transformed into specific emissions (g/kWh) by means of the factory AVL calibration.

2.2 Fuels and delivery

Considering the combustion strategy proposed, the experimental tests were carried out using commercially available diesel and 98 ON gasoline as high and low reactivity fuel, respectively. Their main properties related with auto-ignition are listed in Table 2.

To enable RCCI operation the engine was equipped with a double injection system, one for each different fuel used, as it is shown in the scheme of Figure 2. This injection hardware enables to vary the in-cylinder fuel blending ratio and fuel mixture properties according with the engine operating conditions.

To inject the diesel fuel, the engine was equipped with a common-rail flexible injection hardware which is able to perform up to five injections per cycle; the main characteristic of this hardware is its capability to amplify common-rail fuel pressure for one of the injections by means of a hydraulic piston directly installed inside the injector. The main characteristics of the injector and nozzle used are depicted in Table 3.

Concerning the gasoline injection, an additional fuel circuit was in-house developed with a reservoir, fuel filter, fuel meter, electrically driven pump, heat exchanger and a commercially available port fuel injector (PFI). The mentioned injector was located at the intake manifold and was specified to be able to place all the gasoline fuel into the cylinder during the intake stroke. Consequently, the gasoline injection timing was fixed 10 CAD after the IVO to allow the fuel to flow along 160 mm length (distance from PFI location to intake valves seats). Accordingly, this set up would avoid fuel pooling over the intake valve and the undesirable variability introduced by this phenomenon. The main characteristics of the gasoline injector are depicted in Table 4.

2.3 In-cylinder pressure signal analysis

The combustion analysis was performed with an in-house one-zone model named CALMEC, which is fully described in [30]. This combustion diagnosis tool uses the in-cylinder pressure signal as its main input. The in-cylinder pressure was measured with a Kistler 61215B pressure transducer coupled with a Kistler 5011B10 charge amplifier. A shaft encoder with 1800 pulses per revolution was used, which supplies a resolution of 0.2 CAD. The pressure traces from 150

consecutive engine cycles were recorded in order to compensate the cycle-to-cycle variation during engine operation. Thus, each individual cycle's pressure data was smoothed using a Fourier series low-pass filter. Once filtered, the collected cycles were ensemble averaged to yield a representative cylinder pressure trace, which was used to perform the analysis. Then, the first law of thermodynamics was applied between IVC and EVO, considering the combustion chamber as an open system because of blow-by and fuel injection. The ideal gas equation of state was used to calculate the mean gas temperature in the chamber. Along with these two basic equations, several sub-models were used to calculate instantaneous volume and heat transfer [31], among other things. The main result of the model was the Rate of Heat Release (RoHR). Information related to each cycle can be obtained, such as the IMEP. Start of combustion (SoC) was defined as the crank angle position in which the RoHR slope begins to rise due to combustion and combustion phasing is defined as the crank angle position of 50% fuel mass fraction burned (CA50). Additionally, ringing intensity is calculated by means of the correlation of Eng [32]:

$$RI = \frac{1}{2\gamma}\frac{[0.05 \cdot (dP/dt)_{max}]^2}{P_{max}}\sqrt{\gamma R T_{max}}$$

Where γ is the ratio of specific heats, $(dP/dt)_{max}$ is the peak PRR, P_{max} is the maximum of in-cylinder pressure, R is the ideal gas constant, and T_{max} is the maximum of in-cylinder temperature.

2.4 Computational model description and validation

The computational model was built by means of the CONVERGE CFD code [33]. A reduced reaction mechanism made up of 45 species and 142 reactions [34] including NOx formation (thermal, N_2O and NO_2 pathways) describes the combined oxidation of n-heptane (PRF 0) and iso-octane (PRF 100). The use of these PRF as surrogate fuels is widely accepted to represent the combustion characteristics of diesel and gasoline, respectively [35]-[39]. On the other

hand, the physical properties of diesel fuel are represented by the *diesel2* fuel surrogate available in CONVERGE for spray and mixing process.

The port fuel injected gasoline is considered to be homogeneously mixed and vaporized at IVC and the diesel injection process is simulated by the standard Droplet Discrete Model [40]. Spray atomization and break-up are modeled using the hybrid KH-RT model [41]. Turbulent flow is modeled by means of the RNG k-ε model with wall-functions [41] in order to account for wall heat transfer. Concerning combustion modeling, a direct integration of detailed chemistry approach was used by means of the CONVERGE code and the SAGE solver. A multi-zone model from Babajimopoulos et al.[42] is used to solve the detailed chemistry in zones, i.e., groups of cells that have similar thermodynamic state, in order to speed-up chemistry calculations. Cells are grouped based in two variables, temperature and equivalence ratio. The calculations performed in this project use a 5 K bin size for temperature and 0.01 bin size for equivalence ratio zones. Soot is predicted using a phenomenological soot model [43] based on the approach of Hiroyasu [44].

Calculations run from Intake Valve Close (IVC) with initial thermodynamic conditions as well as wall temperatures estimated from experimental data by means of the in-house combustion diagnostics code CALMEC. Thus, closed-cycle computations on sector grids with periodic boundaries were carried out due to computational efficiency. In these calculations $1/n^{th}$ of the combustion chamber, being *n* the number of nozzle orifices, is modeled. The CFD code uses a structured cartesian grid with base cell size of 1.6 mm. Two additional grid refinements were performed by means of an adaptive mesh refinement (AMR) as well as a fixed refinement within the spray region, as shown in Figure 3.

Figure 4 shows a comparison of the in-cylinder pressure and rate of heat release (RoHR) for the experimental and model predicted results at two different operating conditions (modifying the intake temperature, EGR rate and gasoline percentage in the blend). In addition, the temporal

evolution of HC and CO emissions predicted by the model as well as their experimental measurements are depicted in the figure. The engine operating conditions used to calibrate the computational model are shown in Table 5.

Thus, it can be seen that the model do a reasonable job capturing the combustion characteristics as well as the HC emissions trend and magnitude, however, CO emissions are significantly over-predicted at both operating conditions. Because the simulations reproduce the experimental results well, the simulations are used to understand the combustion efficiency trends observed in Figures 6 and 10.

3. EFFECT OF INTAKE OXYGEN AND TEMPERATURE ON COMBUSTION EFFICENCY

As noted in the introduction section, the in-cylinder equivalence ratios and PRF stratification achieved during RCCI combustion can promote under or over mixing in-chamber regions depending on the operating conditions. It results in higher emissions of unburned HC and CO than traditional mixing-controlled diesel combustion. Moreover, experimental and modelling results have shown that the lowest engine efficiency in RCCI combustion is attained at light loads. These studies demonstrated that the main cause of this reduced engine efficiency was the poor combustion efficiency. Thus, it is interesting to evaluate the influence of different engine settings, specifically the intake oxygen concentration and temperature, in order to determine their influence on the RCCI combustion efficiency at low load.

3.1 Influence of the injection strategy on NOx and soot emissions

This research has been carried out taking into account three main constraints: NOx and soot emissions under EURO VI limits (for HD diesel engines; NOx <0.4 g/kWh and soot <0.01 g/kWh) and ringing intensity (RI) below 5 MW/m^2. Thus, prior to the evaluation of the influence of intake XO_2 and temperature on combustion efficiency, it is necessary to select a proper injection strategy for the high reactivity fuel in order to fulfill these constraints. The engine

operating conditions investigated in this study are shown in Table 6. All the engine settings were held constant except the main direct injection timing in order to study their isolated effect.

Figure 5 presents the results in terms of NOx, soot, unburned HC, CO and combustion efficiency versus the main direct injection timing. In addition, some parameters derived from the combustion event CA50, CA75-CA25, ringing intensity and gross indicated efficiency are depicted. Concerning the specific values shown in Table 6, the pilot direct injection timing was set at -60 CAD ATDC in order to ensure that part of the high reactivity fuel mass had sufficient mixing time prior to the start of combustion to inhibit soot formation. Moreover, it is interesting to note that the values selected for the main direct injection sweep are advanced enough to allow an adequate mixing time for this second fuel mass too, achieving soot levels below the minimum detection limit of the AVL 415S Smoke Meter in all tests. Dashed lines across the figures denote the EURO VI limits for HD diesel engines. On the other hand, it is possible to appreciate how keeping constant all the other engine settings, NOx emissions are strongly dependent on the main direct injection which generates a relatively high reactivity region acting as an ignition source. As the main direct injection timing is delayed, combustion phasing (CA50) is closer to TDC which elevates the combustion temperature. This high temperature achieved during the combustion development enhances the NO formation reactions promoting an increase in the NOx emissions far above of the current regulation limits. In addition, higher levels of ringing intensity appear when the combustion phasing is closer to TDC, but being all the measurements below the 5 MW/m^2 limitation. Thus, it is possible to state that only the most advanced main direct injection settings (-45 and -50 CAD ATDC) are NOx and soot EURO VI compliant. Focusing on the evolution of the unburned HC and CO emissions, it is possible to explain that this improvement in NOx emissions is achieved by deteriorating the fuel oxidation. The poor oxidation process penalizes the combustion efficiency, which drops below 97% for the cases of -45 and -50 CAD ATDC. Regarding the gross

indicated efficiency, an increase of 1% is achieved in -40 and -35 CAD ATDC compared with the extremes of the range tested. The better combustion phasing (CA50) combined with a shorter combustion duration (CA75-CA25) in these cases contributes to enhance the gross indicated efficiency. Unfortunately, these operating conditions exceed the EURO VI NOx limitation.

In the light of the results presented above, it is possible to summarize that a highly premixed strategy for the high reactivity fuel is necessary to achieve all the constraints taken into account in this research. Thus, both -60/-45 and -60/-50 CAD ATDC strategies enable EURO VI NOx and soot compliant values. Due to the fact that combustion efficiency is very similar for both strategies and -60/-50 CAD ATDC strategy offers greater margin of NOx compared with EURO VI limits, this strategy was selected to carry out the main study of the present work. It is interesting to note that other fixed operating conditions have been tested (i.e. gasoline percentage in the blend and EGR) obtaining similar trends. For the sake of brevity, and being the present a preliminary study, they have not been included.

3.2 Combined Effect of Oxygen concentration and In-Cylinder Fuel Blending (ICFB)

The previous section focused on determining a favorable direct injection strategy for RCCI combustion to fulfill the three constraints proposed in this study. For the selected direct injection strategy (-60/-50 CAD ATDC), CO and unburned HC emission levels are unacceptable considering the current regulations limits. In this sense, one strategy to enhance the CO and unburned HC oxidation is to increase the in-cylinder O_2 concentration (i.e. to reduce the EGR percentage). It is interesting to note that computational and experimental studies have demonstrated that in RCCI combustion, the unburned HC depend more on geometric parameters such as crevices and squish volumes [28], so it is not expected to obtain a high benefit in this sense. The improvement in combustion efficiency at the expense of the EGR reduction without any other modification results in a progressive CA50 advancing, which promotes higher combustion temperatures and increasing NOx emissions. Thus, this section

focuses on evaluate the simultaneous variation of the EGR rate and the gasoline percentage in the blend as a strategy to increase the combustion efficiency while achieving NOx <0.4 g/kWh, soot <0.01 g/kWh and RI <5 MW/m^2. The engine operating conditions investigated in this study are shown in Table 7. All the engine settings were held constant except the EGR rate and the gasoline percentage in the blend, which were modified for each test in order to maintain the CA50 at 5.5 CAD ATDC and a constant IMEP of 8.5 bar. From the study presented in section 3.1, it is clear that this combustion phasing allows NOx emissions under the target level as well as very low ringing intensity. Figure 6 presents the results in terms of NOx, soot, unburned HC, CO and combustion efficiency versus the gasoline percentage in the blend. In addition, ringing intensity, CA50, CA75-CA25 and gross indicated efficiency are also depicted. Note that the EGR rate in each case is shown in the figure.

As can be seen from Figure 6, as the EGR rate is decreased an increase of the percentage of gasoline in the blend is needed in order to keep constant the combustion phasing (CA50). In this sense, as the amount of gasoline injected is increased, the in-cylinder reactivity (cetane number) decreases resulting in a more delayed combustion phasing. Thus, it is possible to keep constant the CA50 with a variation of ± 0.5 CAD while reducing the EGR rate. Thus, the differences found regarding the combustion efficiency can be analyzed without considering the influence of the combustion phasing. Focusing on the combustion efficiency a maximum peak of 98.2% is achieved by combining a 43% of EGR and 70.8% of gasoline. At this point, minimum values of 2.9 g/kWh and 2.8 g/kWh are obtained for unburned HC and CO emissions, respectively. Moreover, the highly premixed strategy selected for the high reactivity fuel allows soot levels below the minimum detection limit of the AVL 415S Smoke Meter in all tests. As expected, NOx emissions show a growing trend as the EGR rate is reduced, however, it is worthy to note that all the operating conditions tested are EURO VI compliant in terms of NOx and soot emissions. As shown in previous studies, the slightly delayed CA50 allows the ringing intensity to remain below the target level. It is possible to see how the gross indicated

efficiency values are well correlated with the combustion efficiency. Thus, a maximum peak of 49% is obtained in the case of the lower combustion losses. Note that the test with 38% EGR and 79.6% of gasoline reach the same maximum peak in the gross indicated efficiency (49%). The slightly lower combustion duration (CA75-CA25) in this case compensates the slightly higher combustion losses obtained in this operating condition. Comparing the tests with the maximum and minimum combustion efficiency (43% and 50% EGR, respectively), it is possible to note a reduction of 6.47 g/kWh (69.8%) and 1.61 g/kWh (35.74%) in CO and unburned HC, respectively. Thus, it is clearly demonstrated that an improvement of 1.4% in combustion efficiency is possible by selecting the proper engine settings. In addition, the greater dependency of CO than unburned HC to the engine settings is confirmed.

To better understand the phenomena that govern the combustion efficiency trends observed in Figure 6, a computational analysis by means of the CFD code is presented. Specifically, the tests achieving the maximum and minimum combustion efficiency (43% and 50% EGR, respectively) have been compared. Figure 7 presents the temporal evolution of the mole fraction of several key combustion species, mean temperature and the rate of heat release predicted by the computational model. The mass flow rate profile for the direct injection and the experimental rate of heat release are also depicted in the figure.

Comparing the two cases studied in Figure 7, it is possible to note that the n-heptane consumption starts almost in the same instant of the cycle in both cases due to the low temperature reactions. These low temperature reactions are clearly denoted by the appearance of formaldehyde (CH_2O). During this low temperature heat release phase a first OH accumulation is observed achieving similar values in these two operating conditions. At this moment iso-octane still remains near its IVC concentration in both cases. After the first low temperature reactions, the thermal ignition of the n-heptane is reached when the favorable chemical kinetics (temperature and equivalence ratio) are attained. In this sense, comparing

the evolution of the n-heptane (left and right) it can be observed the more abrupt change in the slope in the case of 43% EGR when the autoignition of the n-heptane is reached. It explains the faster rate of heat release obtained in this case. Due to the increase in the in-cylinder temperature during the thermal ignition of the n-heptane, the most noticeable iso-octane consumption is appreciated. Also of note looking both figures is that formaldehyde consumption is linked to the iso-octane consumption. In this regard, it is also possible to remark that the iso-octane consumption is slowed down in the case of 50% EGR reaching values near an order of magnitude higher than the case of 43% EGR at the end of the cycle. This fact explains the higher unburned HC values registered in this case. Regarding the CO emissions, its oxidation is clearly enhanced in the case of 43% EGR and linked with the OH consumption, which evolution has a noticeable fall in the 43% EGR case when the peak of CO consumption is observed. By contrast, a smooth fall of the OH profile is observed in the case of 50% EGR. The greater fuel amount burned in the 43% EGR case (slightly higher amount of n-heptane and significant higher amount of iso-octane consumed) results in a higher mean temperature peaks (1742 K vs 1540 K) during the combustion event. The higher in-cylinder temperature in the case of 43% EGR promotes higher NOx emissions as the trend of Figure 6 suggests. Thus, the comparison of the key species evolution for both cases clearly denotes differences during the combustion development, which results in different levels of combustion losses. To better understand the spatial dependencies of these losses, in-cylinder images from the modeling work are presented in Figure 8 (43% EGR, 70.8% gasoline) and Figure 9 (50% EGR, 50% gasoline). These figures show three cut planes coincident with the spray axis, squish and crevice regions colored by temperature, mass fraction of CO, mass fraction of n-heptane and mass fraction of iso-octane.

Focusing on the temperature plot at -29.3 CAD ATDC, in both figures, the squish region has a lower temperature than the rest of the cylinder as a consequence of the n-heptane impact in vapor phase due to the highly advanced injection strategy used (-60/-50 CAD ATDC). During

compression, flow tends to move the fuel from the squish region to the firedeck. Thus, because of the higher reactivity found in the squish and crevice regions provided by the spatial location of the diesel fuel, the ignition occurs in this zone once the proper temperature is achieved. Then, the charge is sequentially consumed from more-to-less reactive regions. Considering the n-heptane plot in both figures, it is possible to see how the ignition pattern is almost equal in both cases. The first peak of n-heptane consumption occurs spatially in the squish region out of the piston bowl. Recall that this peak is delayed in time comparing both cases, specifically in the case of 43% EGR this peak is found at -1.3 CAD ATDC and in the case of 50% EGR at -0.7 CAD ATDC. In addition, higher temperature in the case of 43% EGR is present at this time. The major difference found during the combustion development between both operating conditions is the evolution in the late cycle. Thus, it can be seen that in the case of 50% EGR, the greater mass fraction of unburned iso-octane is found in the centerline and unburned n-heptane is located in the crevice and liner regions. On this concern, in the case of 50% EGR, it is possible to see that n-heptane do not progress from the squish to the crevice regions not releasing enough energy, which results in a rapid temperature fall avoiding the complete CO oxidation in this region. Regarding the unburned iso-octane, the low concentration of n-heptane around the centerline do not allow the combustion progression to this zone. Thus, it is confirmed that spatial stratification in the fuel reactivity is a key factor controlling the energy release of dual-fuel RCCI.

3.3 Combined Effect of Intake Temperature and ICFB

As demonstrated in the simulations in the previous section, the non-progression of the n-heptane combustion through crevice regions, results in a rapid fall of the in-cylinder temperature. This low temperature promotes a high amount of CO and unburned HC emissions in the late cycle. Thus, in order to increase the temperature in these regions with the aim of reducing the combustion losses, a simultaneous variation of the intake temperature and gasoline percentage in the blend is evaluated in this section. The same three constraints

than the previous study have been taken into account. The engine operating conditions investigated in this specific study are shown in Table 8. All the engine settings were held constant except the intake temperature and the gasoline percentage, which were modified for each test in order to maintain the CA50 at 5.5 CAD ATDC and a constant IMEP of 8.5 bar. Figure 10 presents the results in terms of NOx, soot, unburned HC, CO and combustion efficiency versus the gasoline percentage in the blend. In addition, ringing intensity, CA50, CA75-CA25 and gross indicated efficiency are also depicted. The corresponding intake temperature is depicted in each case.

Figure 10, shows that if the intake temperature is increased an increase in the percentage of gasoline it is needed in order to keep constant the combustion phasing (CA50). The combustion efficiency profile shows a maximum peak of 98.1%, achieved for a combination of an intake temperature of 50.2°C and 68.7% of gasoline. At this point, minimum values of 2.81 g/kWh and 3.66 g/kWh are obtained for unburned HC and CO emissions, respectively. In addition, all the operating conditions are EURO VI compliant in terms of NOx and soot, with a growing trend in the NOx emissions as the intake temperature increases. Also of note is the higher sensitivity of CO than unburned HC to the operating conditions. Specifically, the comparison of the tests with the maximum and minimum combustion efficiency (50.2°C and 30°C intake temperature, respectively) reveals a reduction of 3.65 g/kWh (49.9%) and 1.32 g/kWh (31.96%) in CO and unburned HC, respectively. The gross indicated efficiency is clearly correlated with the combustion efficiency, which shows a maximum value of 48.5% for the higher combustion efficiency case. In addition, ringing intensity remains below the target level. Thus, for the operating condition set in this study an improvement of 0.9% in combustion efficiency is possible by combining the effect of the intake temperature and gasoline percentage in the blend. Despite the combustion efficiency values obtained with this strategy are similar than the ones obtained through the combination of the EGR and gasoline percentage, it is worthy to note the differences in the CO results. In this sense, the CO trend in

Figure 10 remains almost constant once the intake temperature has exceeded 40°C, not achieving a noticeable benefit.

The computational analysis of the tests achieving the maximum and minimum combustion efficiency in this study (50.2 °C and 30 °C intake temperature, respectively) are presented in Figure 11. As in the previous study, the temporal evolution of the mole fraction of several key combustion species, mean temperature and the rate of heat release predicted by the model are presented. The mass flow rate profile for the direct injection and the experimental rate of heat release are also depicted in the figure.

Comparing the two cases studied in Figure 11 it is possible to see that the low temperature reactions starts almost in the same instant of the cycle denoted by the first n-heptane consumption as well as the appearance of formaldehyde (CH_2O). This first n-heptane consumption in the case of 30 °C intake temperature takes place around -13.5 CAD ATDC, being the case of 50.2 °C intake temperature slightly advanced (-15.8 CAD ATDC). Note that the starting level of n-heptane is different due to the different in-cylinder fuel blending. As commented above, during this LTHR phase a first OH accumulation is observed achieving similar values in these two operating conditions. In addition, iso-octane still remains near its IVC concentration in both cases at this moment. It is interesting to note that similar amounts of n-heptane consumption are found during these first reactions (from SoC to the thermal ignition of the n-heptane). In detail, 21.3% and 24% n-heptane is consumed in this phase for the case of 30 °C and 50.2 °C intake temperature, respectively. Due to the increase in the in-cylinder temperature as a consequence of the first low temperature reactions, the thermal ignition of the n-heptane occurs. This behavior is identified as a change in the n-heptane profile slope, occurring when the mean temperature reach 1200 K approximately in both cases. In this regard, comparing the evolution of the n-heptane (left and right) once the mean temperature arrived to 1200 K it can be observed the most abrupt change in the slope in the

case of 50.2 °C intake temperature. Focusing on the case of 30 °C intake temperature, and comparing the simulated and experimental RoHR profile, it is possible to state that the computational model do not capture with enough accuracy the chemical kinetics in this case. In this sense, these differences between the simulated and experimental RoHR are associated to the slow thermal ignition of the n-heptane in this case, resulting in low in-cylinder temperatures which inhibit to burn the iso-octane. Also of note is that formaldehyde consumption is linked to the iso-octane consumption. In this regard, is possible to appreciate that the iso-octane consumption is slowed down in the case of 30 °C intake temperature reaching values various orders of magnitude higher than the case of 50.2 °C intake temperature at the end of the cycle. This fact explains the higher unburned HC values registered in this case. Regarding the CO emissions, its oxidation is clearly enhanced in the case of 50.2 °C intake temperature case. Moreover, the CO oxidation is linked with the OH consumption which evolution has a noticeable fall in 50.2 °C intake temperature case when the peak of CO consumption is observed. By contrast, a smooth falling of the OH profile is observed in the case of 30 °C intake temperature. As done in the previous study, to better understand the spatial dependencies of these losses, in-cylinder images from the modeling work are presented in Figure 12 (50.2 °C intake temperature, 68.7% gasoline) and Figure 13 (30 °C intake temperature, 50.3% gasoline). These figures show three cut planes coincident with the spray axis, squish and crevice regions colored by temperature, mass fraction of CO, mass fraction of n-heptane and mass fraction of iso-octane.

The highly advanced injection strategy (-60/-50 CAD ATDC) set in these tests results in the wall impact of the n-heptane vapor phase, as the temperature plot at -29.3 CAD ATDC in both figures denotes. Thus, the squish region has a lower temperature than the rest of the cylinder. Considering the n-heptane plot in both figures, it is possible to state how the ignition pattern is almost equal in both cases. The first peak of n-heptane consumption occurs spatially in the squish region out of the piston bowl in both cases. As described in the previous section, this

behavior is explained by the air flow movement during compression stroke, which tends to move the fuel from the squish region to the firedeck. The higher reactivity found in the squish and crevice regions provided by the spatial location of the diesel fuel, makes the ignition occurs in this zone once the proper conditions are achieved. Specifically in the case of 50.2 °C intake temperature the SoC is found at -2.5 CAD ATDC and in the case of 30 °C intake temperature at +1.1 CAD ATDC. Then, the charge is sequentially consumed from more-to-less reactive regions. As found in the previous study, the more noticeable difference noticed during the combustion development between both operating conditions is the evolution in the late cycle. In the case of 30 °C intake temperature, a greater mass fraction of unburned n-heptane is located in the centerline and liner regions. The unburned n-heptane do not trigger the iso-octane combustion contributing to the CO and HC emissions.

4. DISCUSSION

Once a detailed comparison between the tests with the maximum and minimum thermal efficiency obtained for each strategy studied to reduce the combustion losses have been carried out, a direct comparison between both strategies is done in this section. In order to assess the compliance of each strategy with respect to the constraints imposed along the study, a merit function [45] was used. Thus, the constraints taken into account in the calculation of the merit function are EURO VI limits for pollutant emissions (NOx <0.4 g/kWh, soot <0.01 g/kWh, CO <1.5 g/kWh, HC <0.13 g/kWh) and ringing intensity below 5 MW/m^2. The contribution to the merit function (MF) from a given variable will be zero if only the measured value is less than or equal to the specified limit. When F is non-zero, the contribution from each constrained parameter can be examined separately to quantify the severity of its non-compliance. The merit function is defined as follows:

$$F = \sum_i max\left(0, \frac{x_i}{x_i^*} - 1\right)$$

Where F is the merit function, x_i is the value of the i^{th} constrained parameter at the given conditions, x_i* is the constraint of the i^{th} parameter and i is the index over all of the constraints.

Considering that all the tests presented in this research are NOx and soot EURO VI compliant and their ringing intensity are below the target limit, the trend of the merit function is determined by the evolution of the CO and HC emissions, i.e. the evolution of the combustion losses. Focusing on Figure 14 it is interesting to note that the merit function trend is equal for both strategies (EGR+ICFB or T+ICFB), which reveals that the trend in the combustion losses is mainly associated to the in-cylinder equivalence ratio stratification. In this case, the in-cylinder equivalence ratio stratification is determined by the diesel to gasoline ratio in the blend, since the injection timing is kept constant for all the tests. The starting point of 50% ICFB presents the higher combustions losses. As the gasoline mass percentage in the blend is increased a reduction in the combustion losses is obtained. In this sense, regardless of the strategy used (EGR+ICFB or T+ICFB), the minimum combustion losses occurs at around a 70% ICFB. An increase in the gasoline mass percentage to 80% results in a raise in the merit function for both strategies. Analyzing the contribution of each pollutant emission to the merit function, it is possible to confirm that the raise in the MF after 70% ICFB is associated to the increase in HC emissions, while CO remains at the same level as the ICFB 70%. In this case, the low quantity of diesel fuel do not allow the combustion progression to all the premixed regions giving as a result an increase in the HC and CO emissions. Thus, a higher premixed equivalence ratio (from the PFI) improves the combustion development if there is enough high reactivity fuel to trigger the combustion process. Finally, the direct comparison of both strategies along the whole sweep reveals a slight reduction in the combustion losses using the combined effect of intake temperature and ICFB over the use of the combined effect of oxygen concentration and ICFB. The maximum benefit is observed in the case of the 50% ICFB.

5. CONCLUSIONS

In the present study, the influence of the oxygen concentration and intake temperature on RCCI combustion efficiency at light load has been studied combining theoretical and practical tools. An analysis of the parameters derived from a single-cylinder heavy-duty engine in-cylinder pressure measurement has been combined with 3D computational model calculations. In addition to the temporal evolution of several key combustion species, mean temperature and the rate of heat release obtained from the model, spatial in-cylinder images from the modeling work are presented in order to better understand the spatial dependencies of the trends found during the experimental tests.

From the first study, a highly premixed injection strategy (-60/-50 CAD ATDC) for the high reactivity fuel proved to be proper to achieve NOx and soot emissions under EURO VI limits and ringing intensity below the target limit. In this sense, the pilot direct injection timing at -60 CAD ATDC ensures that part of the high reactivity fuel mass had sufficient mixing time prior to the start of combustion to inhibit soot formation. In addition, the main direct injection timing was set to provide a combustion phasing (CA50) around 5.5 CAD ATDC to ensure low combustion temperatures avoiding the NO formation and decreasing NOx emissions.

The combined effect of intake temperature and ICFB resulted in a maximum and minimum combustion efficiency of 98.2% and 96.8% while the use of the combined effect of intake temperature and ICFB allows maximum and minimum values of 98.1% and 97.2%, respectively. By means of the 3D computational simulations it can be stated, for both strategies, how the early injection together with the air flow movement results in a great n-heptane mass fraction located in the crevices and squish regions occurring the first peak of n-heptane consumption in these zones once the proper conditions are achieved. Then, the charge is sequentially consumed from more-to-less reactive regions. In the cases with low combustion efficiency it is possible to note how the n-heptane consumption do not progress from the squish to the

crevice regions not releasing enough energy, which results in a rapid temperature fall avoiding the complete CO oxidation in this region. In addition, greater mass fraction of iso-octane is unburned in this cases due to the low concentration of n-heptane around the centerline, which avoids the combustion progression until this zone.

Finally, the direct comparison of both strategies along the whole sweep suggests that the combustion losses trend is mainly associated to the in-cylinder equivalence ratio stratification, which in this study is determined by the diesel to gasoline ratio in the blend since the injection timing is kept constant for all the tests. Moreover, a slight improvement in the combustion losses using the combined effect of intake temperature and ICFB over the use of the combined effect of oxygen concentration and ICFB is attained.

ACKNOWLEDGMENTS

The authors gratefully acknowledge the modelling support and guidance of José Manuel Pastor and VOLVO Group Trucks Technology for supporting this research.

REFERENCES

[1] Yanagihara H, Sato Y, Minuta J. A simultaneous reduction in NOx and soot in diesel engines under a new combustion system (Uniform Bulky Combustion System e UNIBUS), in: 17th International Vienna Motor Symposium, pp. 303-314, 1996.

[2] Wu H-W, Wang R-H, Ou D-J, Chen Y-C, Chen T-Y. Reduction of smoke and nitrogen oxides of a partial HCCI engine using premixed gasoline and ethanol with air. Applied Energy, Vol. 88, pp 3882-3890, 2011.

[3] Maurya R K, Agarwal A K. Experimental study of combustion and emission characteristics of ethanol fuelled port injected homogeneous charge compression ignition (HCCI) combustion engine. Applied Energy, Vol. 88, pp 1169-1180, 2011.

[4] Lu X, Han D, Huang Z. Fuel design and management for the control of advanced compression-ignition combustion modes. Progress in Energy and Combustion Science, 37, 2011:741-783.

[5] Mingfa Y, Zhaolei Z, Haifeng L. Progress and recent trends in homogeneous charge compression ignition (HCCI) engines. Progress in Energy and Combustion Science 35 (5) (October 2009) 398-437.

[6] Cerit M, Soyhan H S. Thermal analysis of a combustion chamber surrounded by deposits in an HCCI engine. Applied Thermal Engineering 50 (1) (2013) 81-88.

[7] Kiplimo R, Tomita E, Kawahara N, Yokobe S. Effects of spray impingement, injection parameters, and EGR on the combustion and emission characteristics of a PCCI diesel engine, Applied Thermal Engineering 37 (May 2012) 165-175.

[8] Singh A P, Agarwal A K. Combustion characteristics of diesel HCCI engine: an experimental investigation using external mixture formation technique. Appl Energy 2012.

[9] Law D, Kemp D, Allen J, Kirkpatrick G, Copland T. Controlled combustion in an IC-engine with a fully variable valve train. SAE paper 2001-01-0251; 2001.

[10] Agrell F, Ångström H-E, Eriksson B, Wikander J, Linderyd J. Integrated simulation and engine test of closed loop HCCI control by aid of variable valve timings. SAE paper 2003-01-0748; 2003.

[11] Haraldsson G, Tunestål P, Johansson B, Hyvönen J. HCCI combustion phasing in a multi cylinder engine using variable compression ratio. SAE paper 2002-01-2858; 2002.

[12] Maurya R K, Agarwal A K. Experimental investigation on the effect of intake air temperature and air–fuel ratio on cycle-to-cycle variations of HCCI combustion and performance parameters. Applied Energy, Vol. 88, pp 1153-1163, 2011.

[13] Bessonette P W, Schleyer C H, Duffy K P, Hardy W L, Liechty M P. Effects of fuel property changes on heavy-duty HCCI combustion. SAE paper 2007-01-0191, 2007.

[14]Hardy W. An Experimental Investigation of Advanced Diesel Combustion Strategies for Emissions Reductions in a Heavy-Duty Diesel Engine at High Speed and Medium Load. M.S. Thesis, University of Wisconsin - Madison, 2005.

[15]Opat R, Ra Y, Gonzalez M A, Krieger R, Reitz R D, Foster D E, Siewert R, Durrett R. Investigation of mixing and temperature effects on HC/CO emissions for highly dilute low temperature combustion in a light duty diesel engine. SAE paper 2007-01-0193, 2007.

[16]Yang J, Culp T, Kenney T. Development of a Gasoline Engine System Using HCCI Technology e the Concept and the Test Results, SAE paper 2002-1-2832.

[17]Kalghatgi G T, Kumara Gurubaran R, Davenport A, Harrison A J, Hardalupas Y, Taylor AMKP. Some advantages and challenges of running a Euro IV, V6 diesel engine on a gasoline fuel. Fuel, Vol. 108, pp 197-207, 2013.

[18]Yu C, Wang J, Wang Z, Shuai S. Comparative study on Gasoline Homogeneous Charge Induced Ignition (HCII) by diesel and Gasoline/Diesel Blend Fuels (GDBF) combustion. Fuel, Vol. 106, pp 470-447, 2013.

[19]Kalghatgi G, Risberg P, Ångström H. Partially Pre-Mixed Auto-Ignition of Gasoline to Attain Low Smoke and Low NOx at High Load in a Compression Ignition Engine and Comparison with a Diesel Fuel. SAE Technical Paper 2007-01-0006, 2007, doi:10.4271/2007-01-0006.

[20]Hanson R, Splitter D, Reitz R. Operating a Heavy-Duty Direct-Injection Compression-Ignition Engine with Gasoline for Low Emissions. SAE Technical Paper 2009-01-1442, 2009, doi:10.4271/2009-01-1442.

[21]Lewander C M, Johansson B, Tunestal P. Extending the Operating Region of Multi-Cylinder Partially Premixed Combustion using High Octane Number Fuel. SAE Paper 2011-01-1394; 2011.

[22]Kalghatgi G T. Auto-ignition quality of practical fuels and implications for fuel requirements of future SI and HCCI engines. SAE paper 2005-01-0239, 2005.

[23]Kalghatgi G, Risberg P, Angstrom H. Advantages of fuels with high resistance to autoignition in late-injection, low-temperature, compression ignition combustion. SAE Trans., 2006, 115(4), 623–634.

[24]Liu H, Yao M, Zhang B, Zheng Z. Effects of inlet pressure and octane numbers on combustion and emissions of a homogeneous charge compression ignition (HCCI) engine. Energy and Fuels, 2008, 22(4), 2207–2215.

[25]Christensen M, Hultqvist A, Johansson B. Demonstrating the multi-fuel capability of a homogeneous charge compression ignition engine with variable compression ratio. SAE paper 1999-01-3679, 1999.

[26]Splitter D A, Wissink M L, Hendricks T L, Ghandhi J B, Reitz R D. Comparison of RCCI, HCCI, and CDC Operation from Low to Full Load, THIESEL 2012 Conference on Thermo- and Fluid Dynamic Processes in Direct Injection Engines, 2012.

[27]Kokjohn S L, Hanson R M, Splitter D A, Reitz R D. Fuel reactivity controlled compression ignition (RCCI): a pathway to controlled high-efficiency clean combustion, International Journal of Engine Research, 2011.

[28]Splitter D A, Kokjohn S L, Wissink M L, Reitz R. Effect of compression ratio and piston geometry on RCCI load limits and efficiency. SAE technical paper 2012-01-0383; 2012. http://dx.doi.org/10.4271/2012-01-0383.

[29]Dec J E, Yang Y. Boosted HCCI for high power without engine knock and with ultra-low NOx emissions using conventional gasoline. SAE Int. J. Engines, 2010, 3(1), 750–767.

[30]Lapuerta M, Armas O, Hernández J J. Diagnostic of D.I. Diesel Combustion from In-Cylinder Pressure Signal by Estimation of Mean Thermodynamic Properties of the Gas. Applied Thermal Engineering. Vol 19 Nº 5 p. 513–529; 1999.

[31]Payri F, Molina S, Martín J, Armas O. Influence of measurement errors and estimated parameters on combustion diagnosis. Applied Thermal Engineering Vol 26 Nº 2-3 p. 226–236; 2006.

[32]Eng J. Characterization of pressure waves in HCCI combustion. SAE paper 2002-01-2859, 2002.

[33]Senecal P K, Richards K J, Pomraning E, Yang T, Dai M Z, McDavid R M, Patterson M A, Hou S, Shethaji T. A New Parallel Cut-Cell Cartesian CFD Code for Rapid Grid Generation Applied to In-Cylinder Diesel Engine Simulations. SAE 2007-01-0159, 2007, doi:10.4271/2007-01-0159.

[34]Ra Y, Reitz R D. A reduced chemical kinetic model for IC engine combustion simulations with primary reference fuels. Combust. Flame, 2008, 155(4), 713–738.

[35]Ra Y, Reitz R D. The application of a multicomponent droplet vaporization model to gasoline direct injection engines. Int. J. Engine Res., 2003, 4(3), 193–218.

[36]Kokjohn S, Hanson R, Splitter D, Reitz R. Experiments and Modeling of Dual-Fuel HCCI and PCCI Combustion Using In-Cylinder Fuel Blending. SAE Int. J.Engines 2(2):24-39, 2010, doi:10.4271/2009-01-2647.

[37]Kokjohn S, Hanson R, Splitter D, Kaddatz J, et al. Fuel Reactivity Controlled Compression Ignition (RCCI) Combustion in Light- and Heavy-Duty Engines. SAE Int. J.Engines 4(1):360-374, 2011, doi:10.4271/2011-01-0357.

[38]Hanson R M, Kokjohn S L, Splitter D A, Reitz R D. An experimental investigation of fuel reactivity controlled PCCI combustion in a heavy-duty engine. SAE paper 2010-01-0864, 2010.

[39]Splitter D A, Hanson R M, Kokjohn S L, Rein K, Sanders S, Reitz R. D. An optical investigation of ignition processes in fuel reactivity controlled PCCI combustion. SAE paper 2010-01-0345, 2010.

[40]Dukowicz J. A particle fluid numerical model for liquid sprays. J. Comput. Phys., vol. 2, pp. 111–566, 1980.

[41]Han Z, Reitz R D. A Temperature Wall Function Formulation for Variable Density Turbulence Flow with Application to Engine Convective Heat Transfer Modeling. Int. J. Heat and Mass Transfer, Vol. 40, 1997.

[42]Babajimopoulos A, Assanis D N, Flowers D L, Aceves S M, Hessel R P. A fully coupled computational fluid dynamics and multi-zone model with detailed chemical kinetics for the simulation of premixed charge compression ignition engines. International Journal of Engine Research, Vol. 6, 2005.

[43]Kong S-C, Sun Y, Reitz R D. Modeling Diesel Spray Flame Lift-Off, Sooting Tendency and NOx Emissions using Detailed Chemistry with a Phenomenological Soot Model. ASME Journal of Gas Turbines and Power, 2007, 129 245-251.

[44]Hiroyasu H, Kadota T. Models for Combustion and Formation of Nitric Oxide and Soot in Direct Injection Diesel Engines. SAE Technical Paper 760129, 1976, doi: 10.4271/760129.

[45]Cheng, A, Upatnieks A, Mueller C. Investigation of Fuel Effects on Dilute, Mixing-Controlled Combustion in an Optical Direct-Injection Diesel Engine. Energy Fuels, 21 (4), pp 1989–2002, 2007.

ABBREVIATIONS

ATDC: After Top Dead Center

CAD: Crank Angle Degree

CA25: Cranck Angle at 25% mass fraction burned

CA50: Cranck Angle at 50% mass fraction burned

CA75: Cranck Angle at 75% mass fraction burned

CI: Compression Ignition

CR: Compression Ratio

DI: Direct Injection

DPF: Diesel Particulate Filter

EVC: Exhaust Valve Close

EVO: Exhaust Valve Open

FSN: Filter Smoke Number

HCCI: Homogeneous Charge Compression Ignition

HD: Heavy Duty

HT: Heat Transfer

ICE: Internal Combustion Engine

IVC: Intake Valve Close

IVO: Intake Valve Open

LNT: Lean Nox Trap

LTC: Low Temperature Combustion

ON: Octane Number

PFI: Port Fuel Injection

PPC: Partially Premixed Charge

PRF: Primary Reference Fuel

RCCI: Reactivity Controlled Compression Ignition

RoHR: Rate of Heat Release

RI: Ringing Intensity

SI: Spark Ignition

SoC: Start of Combustion

SRC: Selective Catalytic Reduction

TWC: Three-way Catalyst

Engine type	Single cylinder, 4 St cycle, DI
Bore x Stroke [mm]	123 x 152
Connecting rod length [mm]	225
Displacement [L]	1.806
Geometric compression ratio [-]	14.4:1

Bowl Type	Open crater
Number of Valves	4
IVO	375 CAD ATDC
IVC	535 CAD ATDC
EVO	147 CAD ATDC
EVC	347 CAD ATDC

Table 1. Single cylinder engine specifications

	Gasoline	Diesel
Density [kg/m^3] (T= 15 °C)	772	882
Viscosity [mm^2/s] (T= 40 °C)	0.37	2.8
Octane number [-]	98	-
Cetane number [-]	-	52
Lower heating value [kJ/kg]	44.542	42.651

Table 2. Physical and chemical properties of the fuels used along the study

Actuation Type	Solenoid
Steady flow rate @ 100 bar [cm^3/s]	28.56
Number of Holes	7
Hole diameter [µm]	194
Included Spray Angle [°]	142

Table 3. High reactivity fuel injector characteristics

Injector Style	Saturated
Steady flow rate @ 3 bar [cm^3/min]	980
Included Spray Angle [°]	30
Injection Pressure [bar]	5.5
Injection Strategy	Single
Start of Injection Timing	385 CAD ATDC

Table 4. Low reactivity fuel injector characteristics

	Left	Right
Engine speed [rpm]	1200	
Piston Bowl	Open crater	
CR [-]	14.4:1	

Injector Nozzle	7x194-142°	
IMEP [bar]	8.5	
CA50 [CAD ATDC]	5.5 ± 0.5	
Intake Temperature [°C]	40	50.2
EGR [%]	43	46.6
Gasoline percentage [% total]	70.8	68.7
Diesel pilot inj. timing [CAD ATDC]	-60	
Fuel mass in pilot Diesel inj. [%]	50	
Diesel main inj. timing [CAD ATDC]	-50	
Diesel injection pressure [bar]	700	
Gasoline inj. timing [CAD ATDC]	385	
Total fuel mass [mg/cycle]	70	

Table 5. Operating conditions used to calibrate the computational model

Engine speed [rpm]	1200
Piston Bowl	Open crater
CR [-]	14.4:1
Injector Nozzle	7x194-142°
EGR [%]	30
Intake Temperature [°C]	40
Diesel pilot inj. timing [CAD ATDC]	-60
Fuel mass in pilot Diesel inj. [%]	50
Diesel main inj. timing [CAD ATDC]	from -25 to -50
Diesel injection pressure [bar]	700
Gasoline [% mass]	85
Gasoline inj. timing [CAD ATDC]	385
Total fuel mass [mg/cycle]	70

Table 6. Operating conditions tested to evaluate the effect of the high reactivity fuel injection strategy on NOx and soot emissions

Engine speed [rpm]	1200
Piston Bowl	Open crater
CR [-]	14.4:1
Injector Nozzle	7x194-142°

IMEP [bar]	8.5
CA50 [CAD ATDC]	5.5 ± 0.5
Intake Temperature [°C]	40
Diesel pilot inj. timing [CAD ATDC]	-60
Fuel mass in pilot Diesel inj. [%]	50
Diesel main inj. timing [CAD ATDC]	-50
Diesel injection pressure [bar]	700
Gasoline inj. timing [CAD ATDC]	385
Total fuel mass [mg/cycle]	70

Table 7. Operating conditions tested to evaluate the combined effect of the oxygen concentration and gasoline percentage on combustion efficiency

Engine speed [rpm]	1200
Piston Bowl	Open crater
CR [-]	14.4:1
Injector Nozzle	7x194-142°
IMEP [bar]	8.5
CA50 [CAD ATDC]	5.5 ± 0.5
EGR [%]	46.6
Diesel pilot inj. timing [CAD ATDC]	-60
Fuel mass in pilot Diesel inj. [%]	50
Diesel main inj. timing [CAD ATDC]	-50
Diesel injection pressure [bar]	700
Gasoline inj. timing [CAD ATDC]	385
Total fuel mass [mg/cycle]	70

Table 8. Operating conditions tested to evaluate the combined effect of the intake temperature and gasoline percentage on combustion efficiency

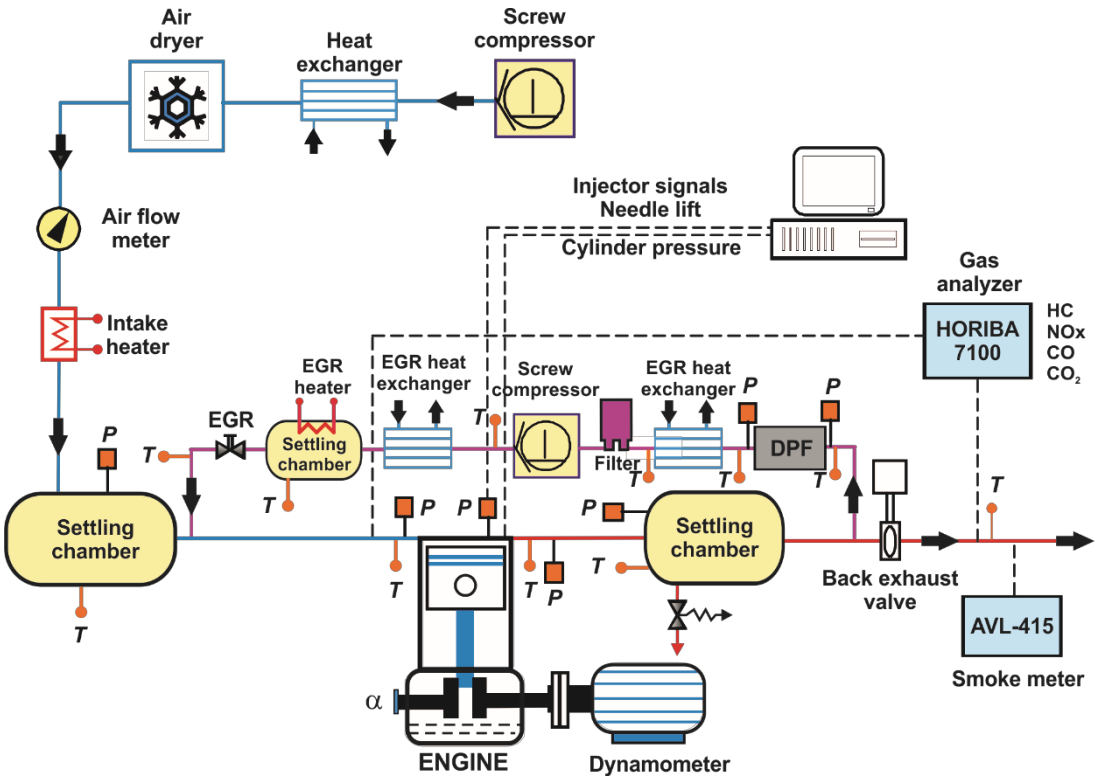

Figure 1. Complete test cell setup.

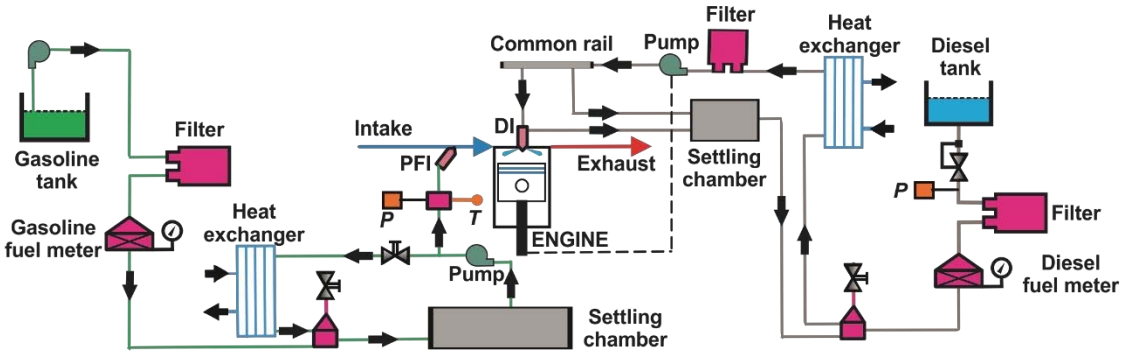

Figure 2. Fuel injection systems scheme.

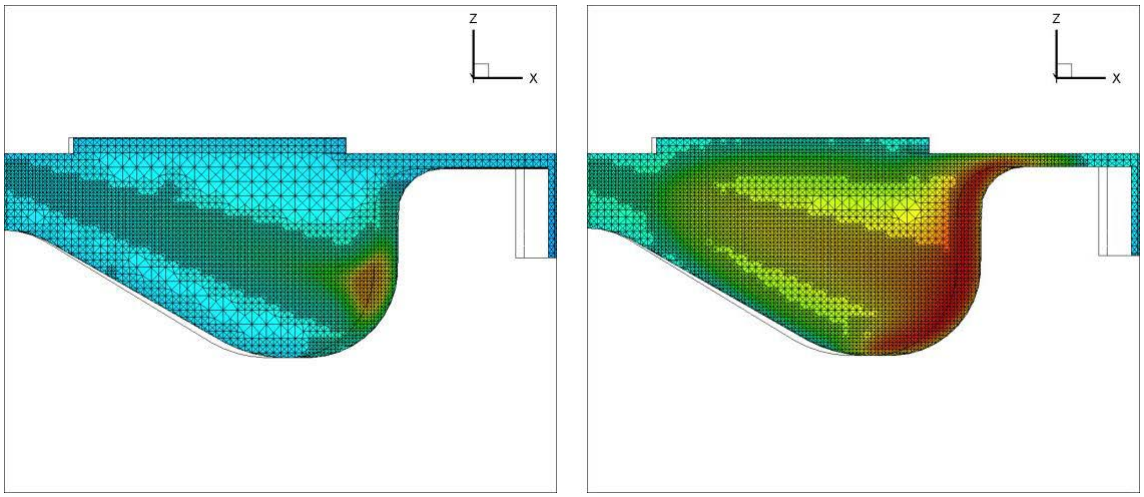

Figure 3. Different grid refinements by CONVERGE adaptive mesh refinement. Left: temperature contours at -5 CAD ATDC. Right: temperature contours at +3 CAD ATDC.

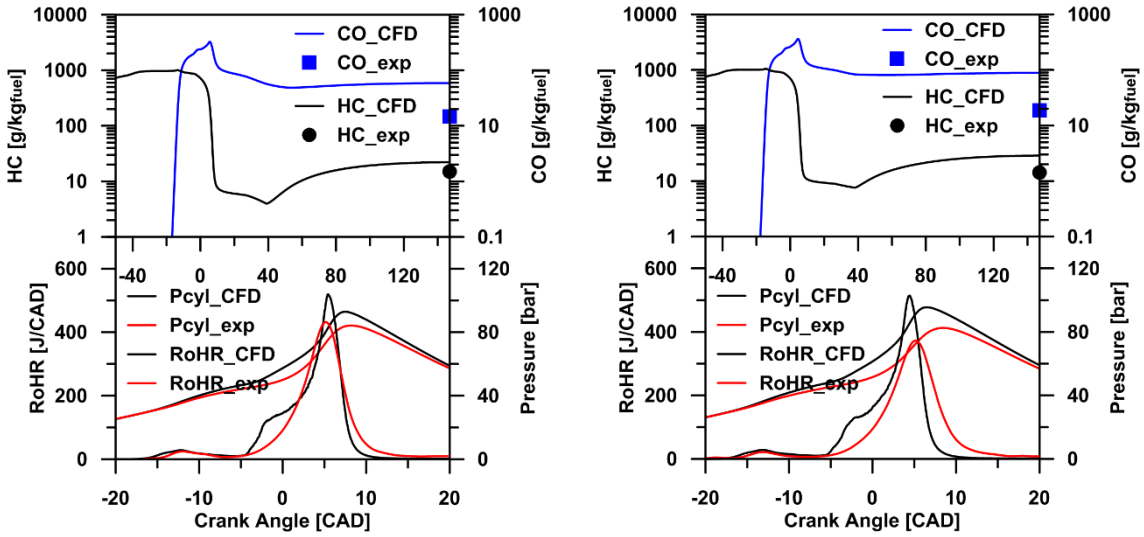

Figure 4. Comparison of the in-cylinder pressure, RoHR, HC and CO for the experimental and model predicted results at the two different operating conditions shown in Table 5.

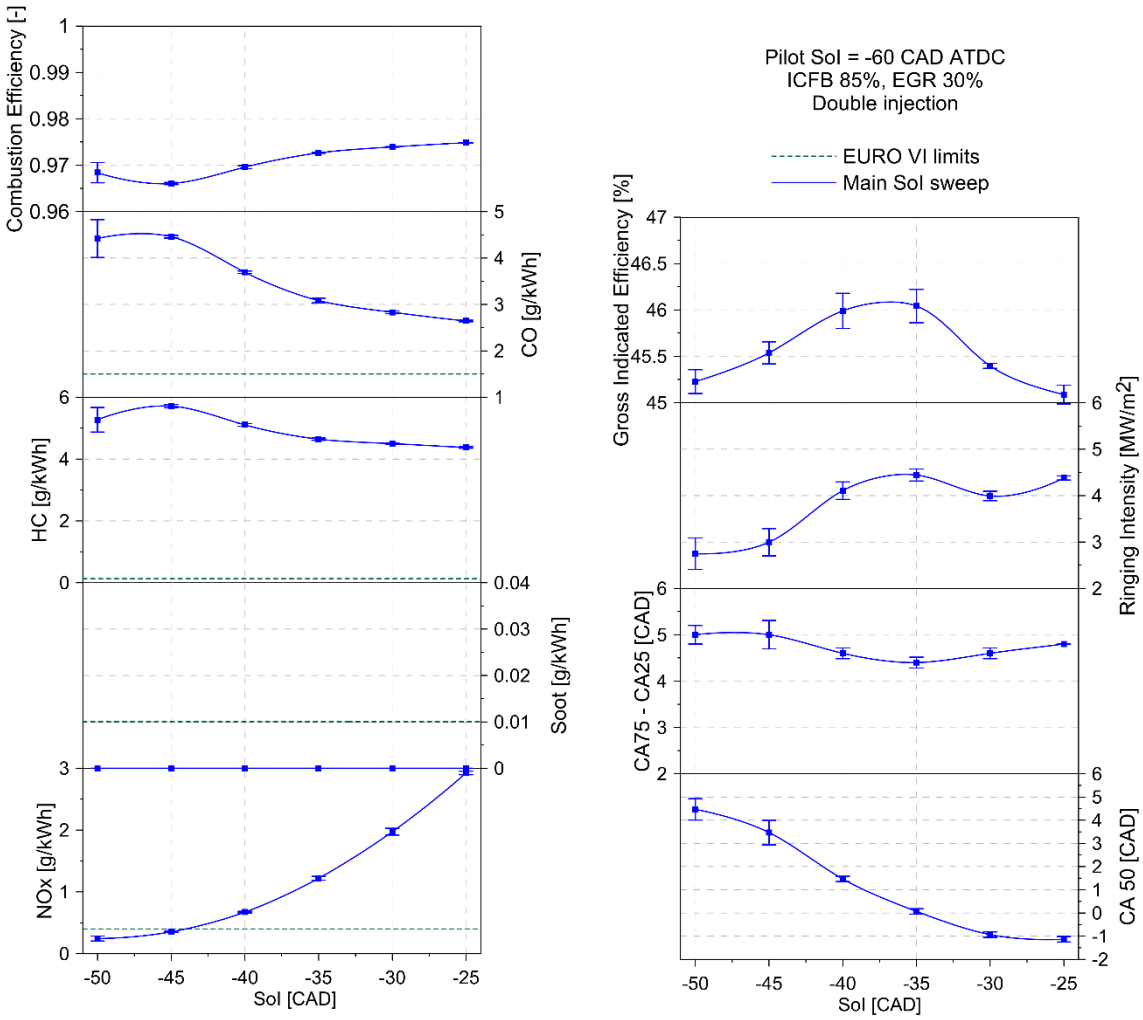

Figure 5. Engine-out emissions and combustion parameters as a function of the second direct injection timing.

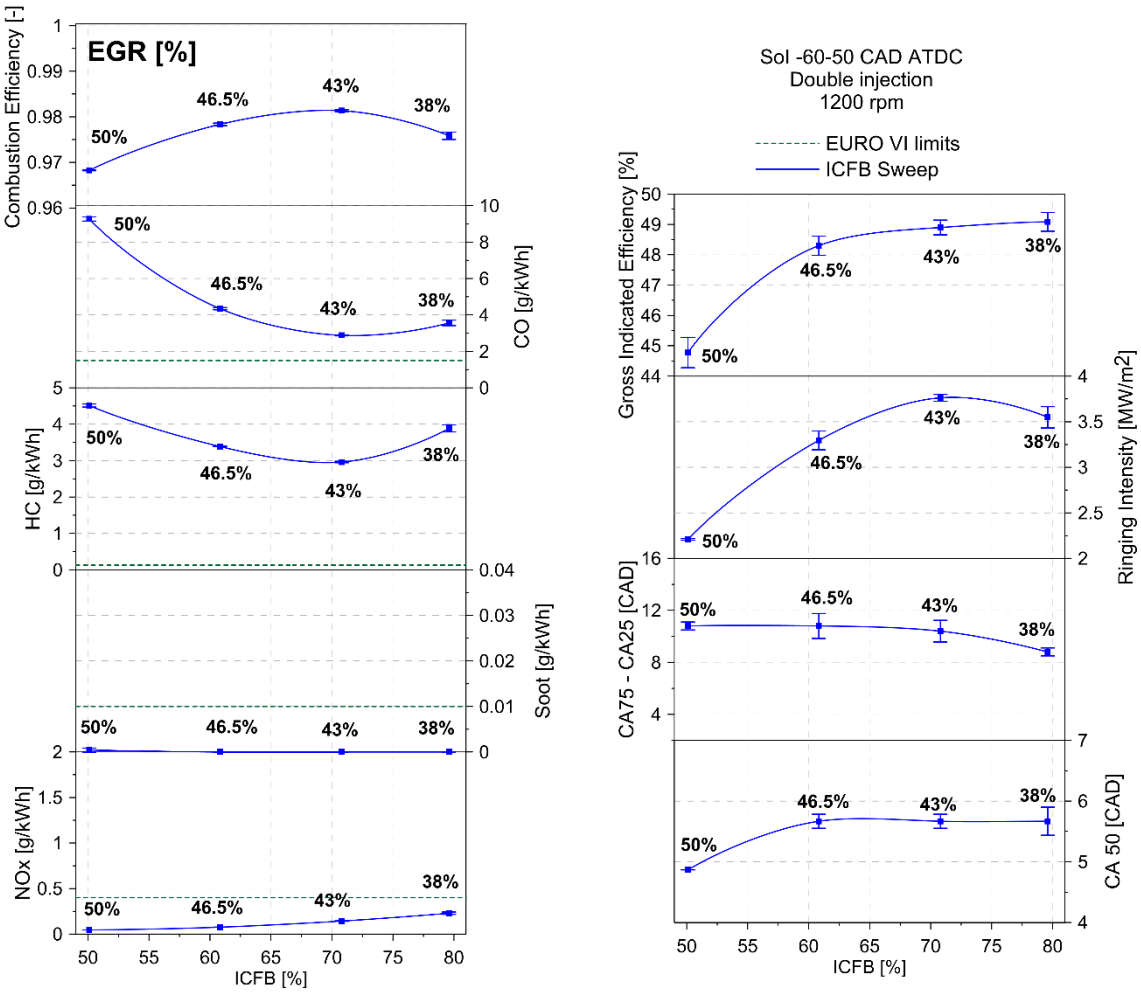

Figure 6. Engine-out emissions and combustion parameters as a function of the gasoline percentage in the blend.

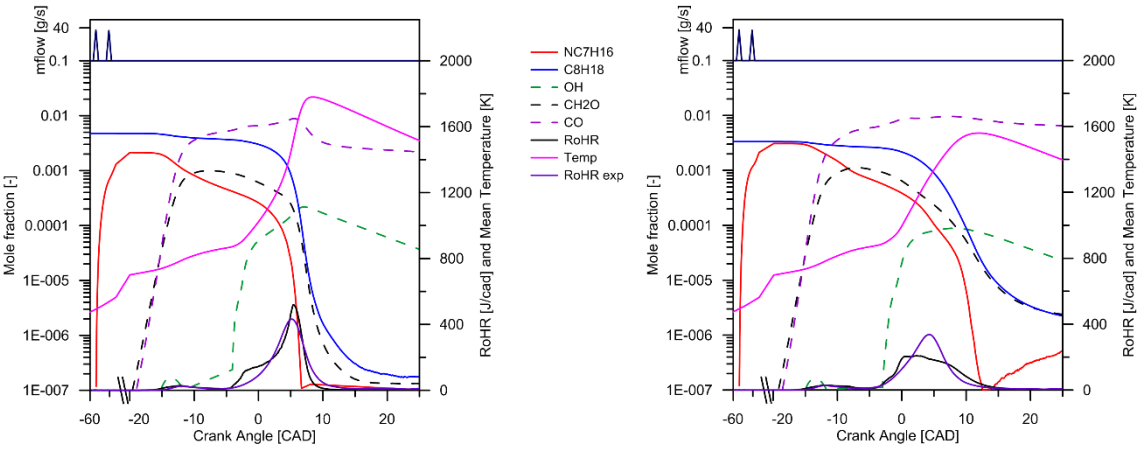

Figure 7. Evolution of several key combustion species, mean temperature and the simulated and experimental rate of heat release for the cases of the maximum (left: 43% EGR, 70.8% gasoline) and minimum (right: 50% EGR, 50% gasoline) combustion efficiency.

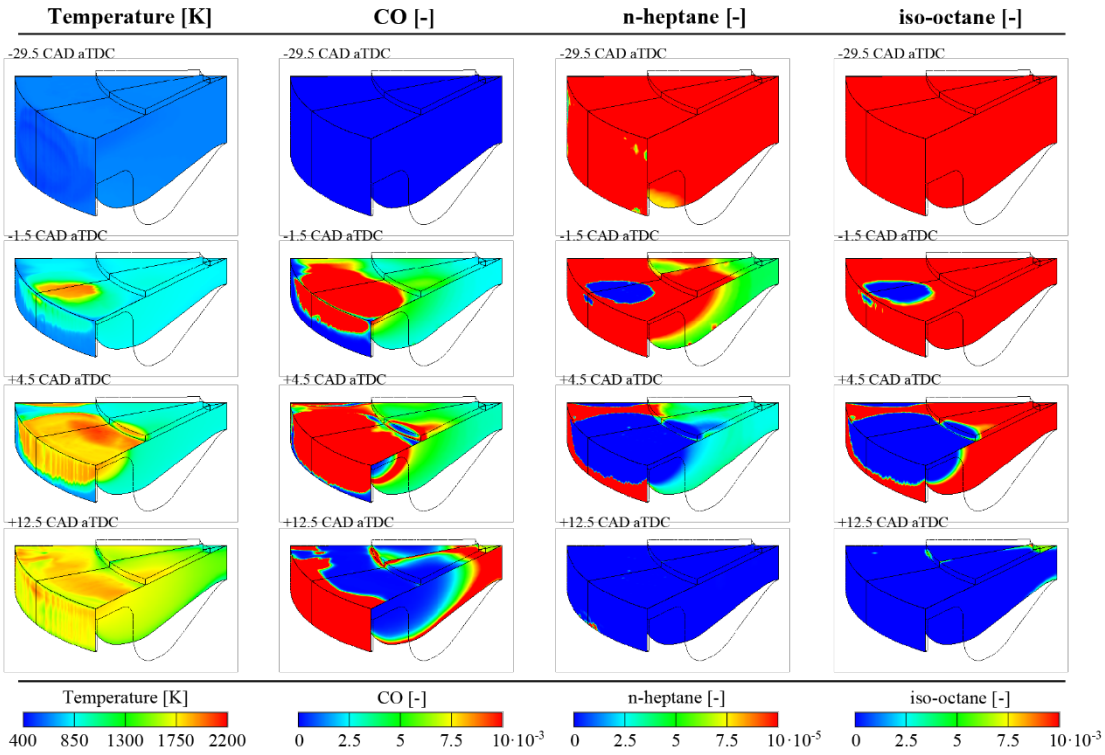

Figure 8. Cut planes coincident with the spray axis, squish and crevice regions colored by temperature, mass fraction of CO, mass fraction of n-heptane and mass fraction of iso-octane for the case: 43% EGR, 70.8% gasoline.

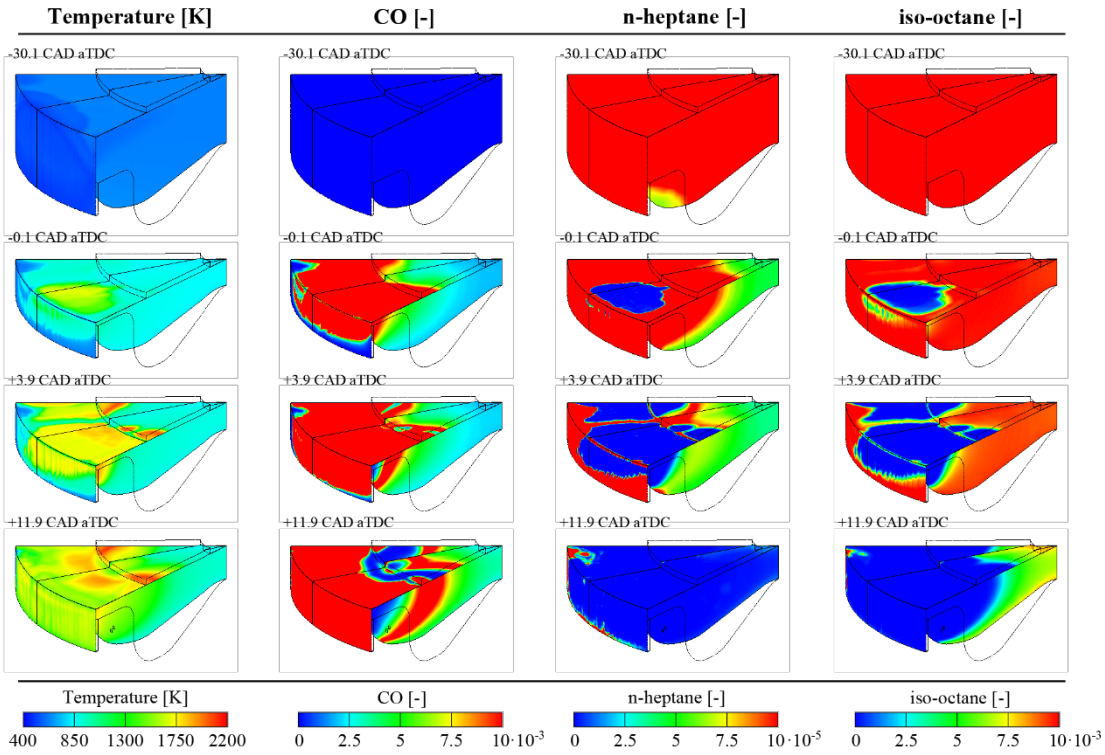

Figure 9. Cut planes coincident with the spray axis, squish and crevice regions colored by temperature, mass fraction of CO, mass fraction of n-heptane and mass fraction of iso-octane for the case: 50% EGR, 50% gasoline.

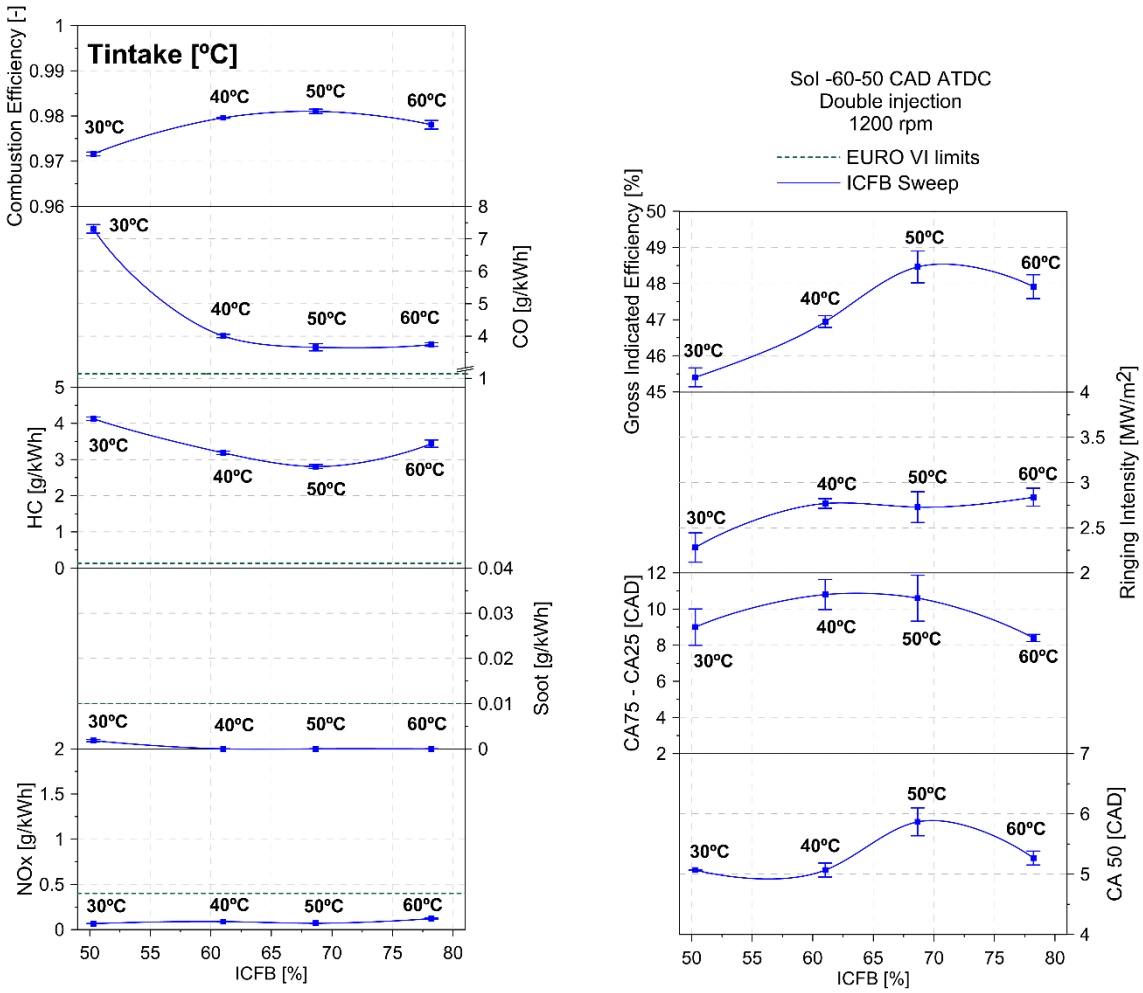

Figure 10. Engine-out emissions and combustion parameters as a function of the gasoline percentage in the blend.

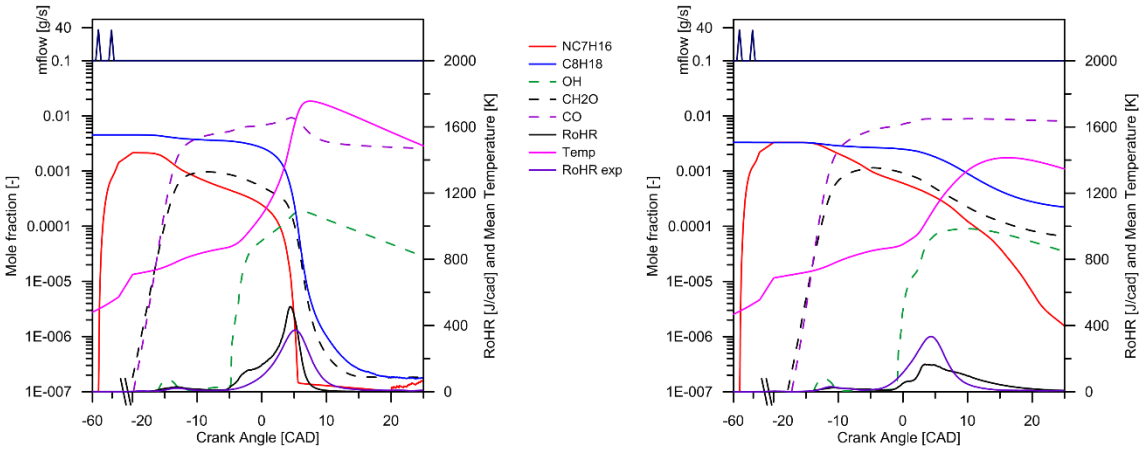

Figure 11. Evolution of several key combustion species, mean temperature and the simulated and experimental rate of heat release for the cases of the maximum (left: 50.2 °C intake temperature, 68.7% gasoline) and minimum (right: 30 °C intake temperature, 50.3% gasoline) combustion efficiency.

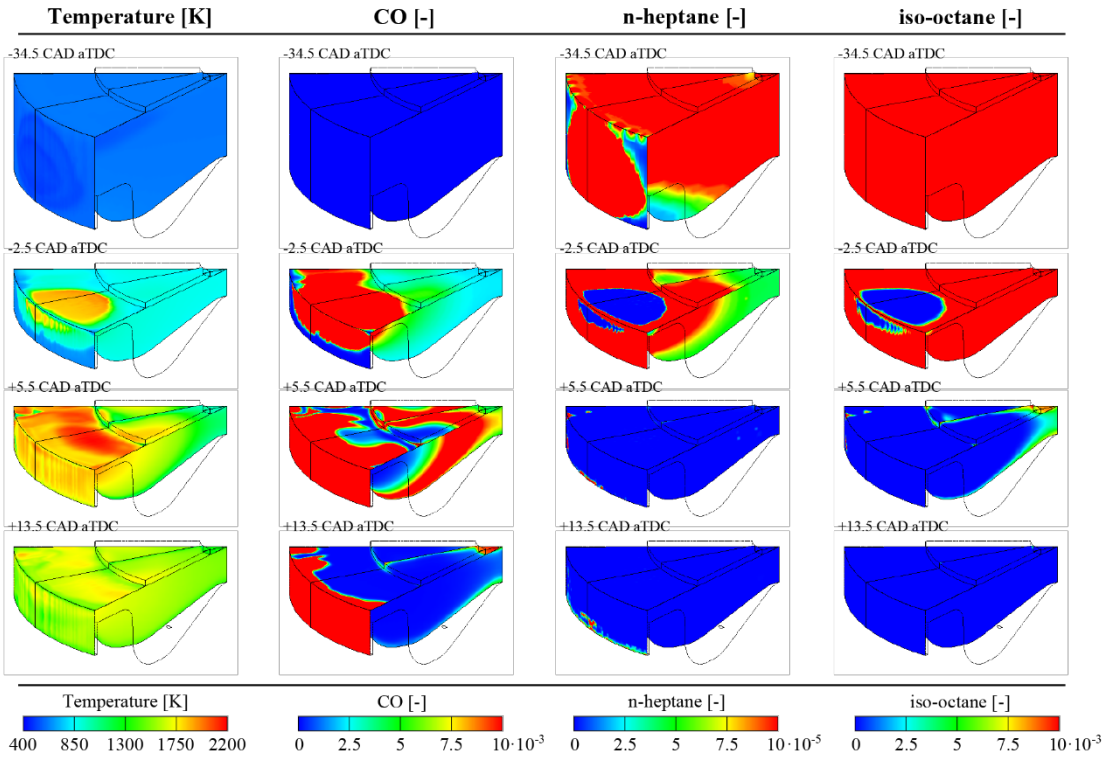

Figure 12. Cut planes coincident with the spray axis, squish and crevice regions colored by temperature, mass fraction of CO, mass fraction of n-heptane and mass fraction of iso-octane for the case: 50.2 °C intake temperature, 68.7% gasoline.

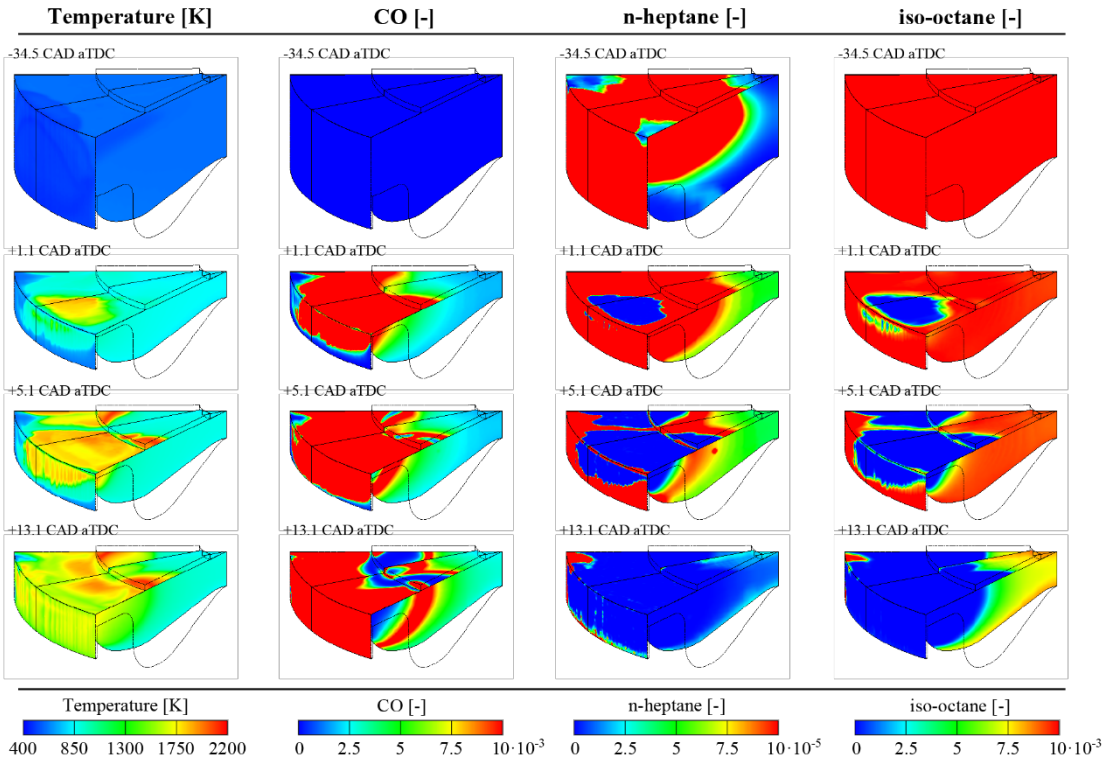

Figure 13. Cut planes coincident with the spray axis, squish and crevice regions colored by temperature, mass fraction of CO, mass fraction of n-heptane and mass fraction of iso-octane for the case: 30 °C intake temperature, 50.3% gasoline.

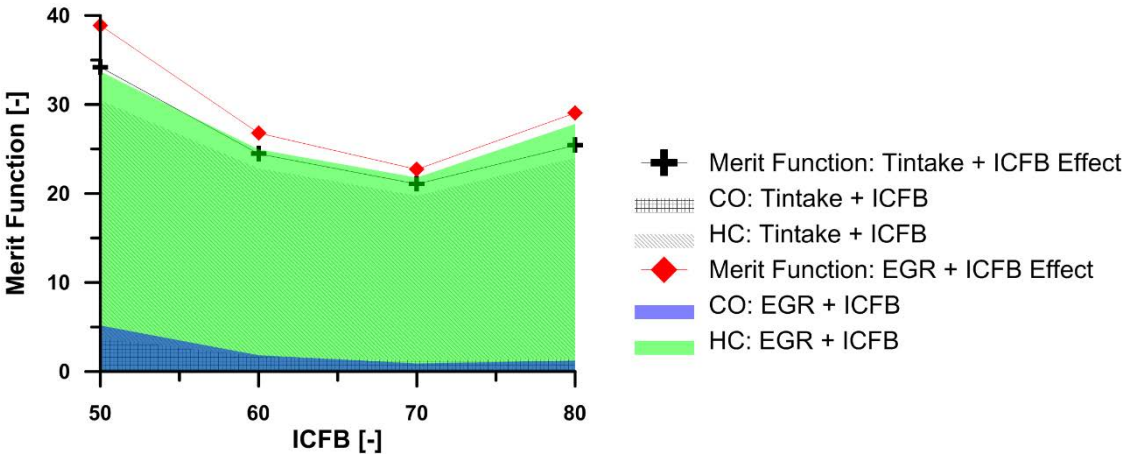

Figure 14. Merit function calculated taking into account (NOx <0.4 g/kWh, soot <0.01 g/kWh and RI < 5 MW/m^2) of the tests carried out to evaluate the strategies studied to reduce the combustion losses (combined Effect of Oxygen concentration and ICFB or combined Effect of Intake Temperature and ICFB).

HIGHLIGHTS

- Advanced split diesel injections allows NOx and soot emissions under EURO VI limits
- Combustion losses reduction by combining the intake temperature and XO_2 with ICFB
- The in-cylinder equivalence ratio stratification governs the combustion losses
- Low intake XO_2 promotes high amount of unburned iso-octane in the centerline
- Unburned n-heptane located in the crevice and liner regions